

On the absence of a spiral magnetic order in Li_2CuO_2 with one-dimensional CuO_2 ribbon chains

H. J. Xiang, C. Lee, and M.-H. Whangbo*

Department of Chemistry, North Carolina State University, Raleigh, North Carolina 27695-8204

(Dated: October 24, 2018)

On the basis of first principles density functional theory electronic structure calculations as well as classical spin analysis, we explored why the magnetic oxide Li_2CuO_2 , consisting of CuO_2 ribbon chains made up of edge-sharing CuO_4 squares, does not exhibit a spiral-magnetic order. Our work shows that, due to the next-nearest-neighbor interchain interactions, the observed collinear magnetic structure becomes only slightly less stable than the spin-spiral ground state, and many states become nearly degenerate in energy with the observed collinear structure. This suggests that the collinear magnetic structure of Li_2CuO_2 is a consequence of order-by-disorder induced by next-nearest-neighbor interchain interactions.

PACS numbers: 75.25.+z, 75.10.Hk, 75.10.Pq, 71.70.Gm

Copper oxides with CuO_2 ribbon chains made up of edge-sharing CuO_4 squares have one-dimensional chains of spin- $\frac{1}{2}$ Cu^{2+} ions, and exhibit unique physical properties. LiCu_2O_2 ¹ and LiCuVO_4 ² show ferroelectricity when their CuO_2 ribbon chains undergo a spiral-magnetic order at low temperatures. For a chain of spin- $\frac{1}{2}$ ions, a spin spiral structure is predicted when the nearest-neighbor (NN) ferromagnetic (FM) spin exchange J_1 and the next-nearest-neighbor (NNN) antiferromagnetic (AFM) spin exchange J_2 satisfy the condition $|J_2/J_1| > 0.25$, while an FM structure is predicted if $|J_2/J_1| < 0.25$.³ The copper oxide Li_2CuO_2 also consists of CuO_2 ribbon chains, but has a different magnetic structure. A neutron powder diffraction study of Li_2CuO_2 at 1.5 K showed a collinear magnetic structure in which the spins of each CuO_2 chain has an FM arrangement with Cu moments perpendicular to the plane of the CuO_2 ribbon and the arrangement between adjacent FM chains is AFM⁴ (hereafter this magnetic structure will be referred to as the AFM-I state). Thus, to explain this collinear magnetic structure, one might expect $|J_2/J_1| < 0.25$ for the CuO_2 chains of Li_2CuO_2 . Indeed, Graaf *et al.* obtained $|J_2/J_1| = 0.15$ on the basis of first principles electronic structure calculations using the embedded cluster model.⁵ However, the CuO_2 ribbon chains of Li_2CuO_2 are similar in structure to those of LiCu_2O_2 and LiCuVO_4 , so that $|J_2/J_1| > 0.25$ would have been expected. If $|J_2/J_1| > 0.25$, one needs to ask why a spiral magnetic order does not occur in Li_2CuO_2 . In addition, more than two spin exchange interactions are necessary to describe the magnetic structure of Li_2CuO_2 , and the nature and magnitude of these interactions are not unequivocal.^{6,7} Another puzzle concerning Li_2CuO_2 is that it undergoes a phase transition below ~ 2.4 K to a state believed to be a spin canted state.^{8,9,10} So far, the origin and the nature of this phase transition remain unclear.

The spiral magnetic order of LiCu_2O_2 and LiCuVO_4 is a consequence of the spin frustration associated with the NN FM and NNN AFM interactions in their CuO_2 chains. A collinear magnetic order can occur as a consequence of order-by-disorder,^{11,12} which occurs typically

in highly spin frustrated systems.¹³ Provided that a spin spiral state is the ground state for the CuO_2 chains of Li_2CuO_2 , one might speculate if the AFM-I state of Li_2CuO_2 is close in energy to the spin spiral state and if Li_2CuO_2 has a large number of nearly degenerate states around the AFM-I state. In the present work we explore these possibilities by studying the magnetic structure of Li_2CuO_2 on the basis of first principles density functional theory (DFT) electronic structure calculations and carrying out classical spin analysis with the spin exchange parameters deduced from the DFT calculations.

TABLE I: Relative energies (in meV/Cu) of the various magnetic states with respect to the FM state obtained from GGA+U calculations with different U_{eff} values.

U_{eff} (eV)	0	2	4	6	8	10
E(AF1)	-9.59	-5.80	-3.84	-2.38	-1.46	-0.96
E(AF2)	0.69	4.89	5.76	5.82	4.70	3.67
E(AF3)	-15.34	-8.01	-4.29	-1.960	-0.71	-0.18
E(AF4)	-6.66	-1.00	1.23	2.23	2.22	1.88
E(AF5)	1.25	5.00	5.77	5.80	4.65	3.65

Our DFT electronic structure calculations employed the full-potential augmented plane wave plus local orbital method as implemented in the WIEN2k code.¹⁴ For the exchange-correlation energy functional, the generalized gradient approximation (GGA)¹⁵ was employed¹⁶ with $R_{MT}^{min}K_{max} = 7.0$. To properly describe the strong electron correlation in the 3d transition-metal oxide, the GGA plus on-site repulsion U method (GGA+U) was employed.¹⁷ We also examined the energy of Li_2CuO_2 as a function of the magnetic order parameter \mathbf{q} by employing the non-collinear magnetism code, WIENncm.¹⁸

Li_2CuO_2 has a body centered orthorhombic structure (space group Immm with $a = 3.654$ Å, $b = 2.860$ Å, and $c = 9.377$ Å),⁴ where the CuO_2 ribbon chains run along the b-direction (Fig. 1). As depicted in Fig. 1a, there are five possible spin exchange interactions to consider; J_1 and J_2 are NN and NNN intrachain interactions, respec-

tively, J_3 and J_4 are NN and NNN interchain interactions along the c -direction, respectively, while J_5 is the interchain interaction along the a -direction. To evaluate the interactions $J_1 - J_5$, we calculate the relative energies of the six ordered collinear spin states shown in Fig. 2 in terms of GGA+U calculations. To see the dependence of these spin exchange interactions on the effective on-site repulsion $U_{eff} = U - J$, our GGA+U calculations were carried out with U_{eff} ranging from 0 to 10 eV. (For 3d transition metals, U is generally less than 10 eV and the J value is usually 1 eV.) The relative energies of the six ordered spin states of Fig. 2 obtained from our GGA+U calculations are summarized in Table I. In terms of the exchange parameters $J_1 - J_5$, the energies of the six magnetic states per Cu are written as

$$\begin{aligned}
 E(FM) &= (J_1 + J_2 + 4J_3 + 4J_4 + J_5)/4 \\
 E(AF1) &= (J_1 + J_2 - 4J_3 - 4J_4 + J_5)/4 \\
 E(AF2) &= (-J_1 + J_2 + J_5)/4 \\
 E(AF3) &= (-J_2 + 2J_3 - 2J_4 + J_5)/4 \\
 E(AF4) &= (-J_1 + J_5)/8 \\
 E(AF5) &= (-J_1 + J_2 - J_5)/8
 \end{aligned}
 \tag{1}$$

Thus, by equating the energy differences of these states in terms of the spin exchange parameters with the corresponding energy differences in terms of the GGA+U calculations, we obtain the values of $J_1 - J_5$ summarized in Table II, where we employed the convention in which positive and negative numbers represent AFM and FM interactions, respectively. J_5 is very weak in agreement with Mizuno *et al.*⁷ The NNN interchain interaction J_4 is much stronger than the NN interchain interaction J_3 , and this finding does not support the assumption by Mizuno *et al.* that J_3 and J_4 are similar.⁷ J_4 is stronger than J_3 because the overlap between the magnetic orbitals, which depends on the overlap between the O 2p orbitals of the magnetic orbitals,¹⁹ is much more favorable for the path J_4 than for the path J_3 (Fig. 3). The NN intrachain interaction J_2 is FM while the NNN intrachain interaction J_1 is FM while the NNN intrachain interaction J_2 is AFM. These intrachain interactions are the same in nature to those reported by Graaf *et al.*⁵ However, our study shows that $|J_2/J_1| > 0.25$, for all U_{eff} values employed, and hence Li_2CuO_2 should have a spin-spiral ground state as far as isolated CuO_2 ribbon chains are concerned.

TABLE II: Calculated exchange parameters (in meV) deduced from GGA+U calculations.

U_{eff} (eV)	0	2	4	6	8	10
J_1	-10.98	-15.58	-15.36	-14.02	-10.86	-8.31
J_2	23.91	15.78	10.44	7.35	4.48	3.00
J_3	1.07	0.34	-0.04	-0.01	-0.09	-0.03
J_4	3.73	2.56	1.95	1.20	0.82	0.51
J_5	-1.12	-0.22	-0.01	0.05	0.09	0.05

To see how the above prediction is affected by the

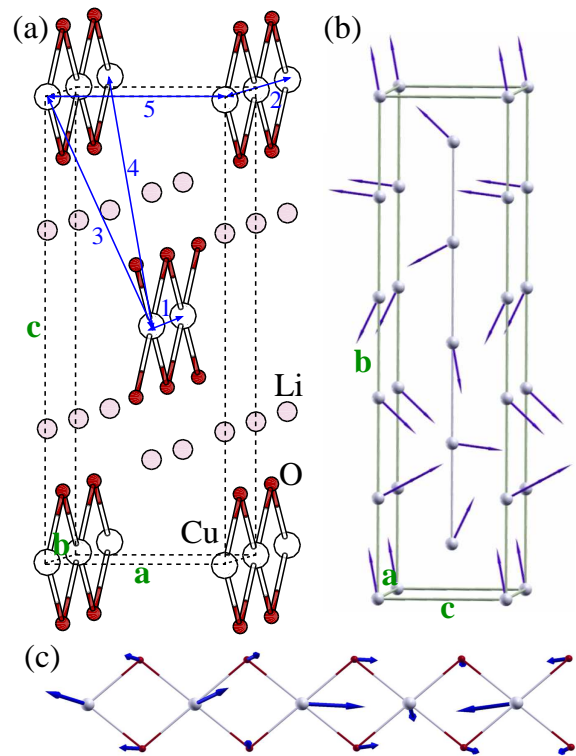


FIG. 1: (Color online) (a) Crystal structure and five spin exchange paths $J_1 - J_5$ of Li_2CuO_2 . (b) Cu moments of the spin spiral ground state at $\mathbf{q} = (0, 0.20, 0)$ obtained from the GGA+U non-collinear calculation with $U_{eff} = 6$ eV. (c) Detailed view of the Cu and O moments of a CuO_2 ribbon chain in the spin spiral ground state shown in (b). For the purpose of illustration, the O moments were increased by three times.

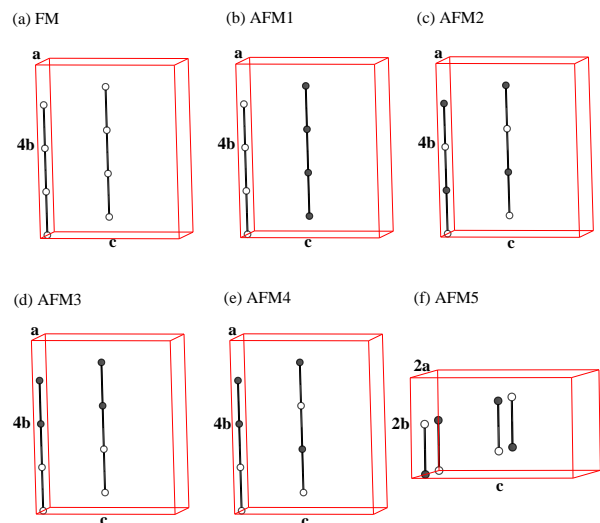


FIG. 2: (Color online) Schematic representations of the six ordered spin arrangements of Li_2CuO_2 employed for GGA+U calculations to extract the five spin exchange parameters $J_1 - J_5$. The filled and empty circles the up-spin and down-spin Cu sites, respectively.

NNN interchain interaction J_4 , we carried out a classical spin analysis based on the Freiser method^{20,21} using the three dominant exchange parameters J_1 , J_2 , and J_4 . The spin interaction energy of an ordered spin state with $\mathbf{q} = (2\pi q_x/a, 2\pi q_y/b, 2\pi q_z/c)$ can be written as

$$E(\mathbf{q}) = J_4 \{ \cos[2\pi(q_x/2 + 3q_y/2 + q_z/2)] + \cos[2\pi(-q_x/2 + 3q_y/2 + q_z/2)] + \cos[2\pi(q_x/2 - 3q_y/2 + q_z/2)] + \cos[2\pi(q_x/2 + 3q_y/2 - q_z/2)] \} + \cos(2\pi q_y) J_1 + \cos(4\pi q_y) J_2. \quad (2)$$

For simplicity of our discussion, we will represent \mathbf{q} by (q_x, q_y, q_z) . This $E(\mathbf{q})$ vs. \mathbf{q} relation has minima along the $(0, q_y, 0)$ direction. The $E(0, q_y, 0)$ vs. $(0, q_y, 0)$ curves calculated with the spin exchange parameters derived from the GGA+U calculations for $U_{eff} = 6$ eV are presented in Fig. 4. The solid curve, obtained only with the intrachain interactions J_1 and J_2 , shows two minima (at $q_y = 0.18$ and $q_y = 0.82$) of equal energy. The FM state ($q_y = 0.00$) and the AFM-I state ($q_y = 1.00$) are identical in energy, and are less stable than the two spin-spiral states ($q_y = 0.18$ and $q_y = 0.82$). These are the expected results in the absence of the interchain interaction because $|J_2/J_1| > 0.25$. The dashed curve, obtained with the intrachain interactions J_1 and J_2 as well as the interchain interaction J_4 , also shows two minima at $q_y = 0.21$ and $q_y = 0.90$. Note that the interchain interaction J_4 raises the energy of the FM state while lowering that of the AFM-I state. As a result, the $E(0, q_y, 0)$ vs. $(0, q_y, 0)$ curve around $q_y = 0.21$ becomes sharper while that around $q_y = 0.90 - 1.00$ is nearly flat. Both spin-spiral states are only slightly more stable than the collinear AFM-I state. Our calculations using the spin exchange parameters obtained with $U_{eff} < 6$ eV show that the energy around $q_y = 0.21$ becomes lower than that around $q_y = 0.90$, and both states have lower energies than the collinear AFM-I state ($q_y = 1.00$). In terms of the parameters obtained for $U_{eff} > 6$ eV, however, the collinear AFM-I state becomes the ground state.

Now we evaluate $E(0, q_y, 0)$ vs. $(0, q_y, 0)$ relations on the basis of non-collinear GGA+U electronic structure calculations using the WIENncm code.¹⁸ In this method, the incommensurate spiral magnetic order is simulated without resorting to the supercell technique by using the generalized Bloch theorem.²² The $E(0, q_y, 0)$ vs. $(0, q_y, 0)$ relation calculated for the representative U_{eff} (i.e., 6 eV), presented in Fig. 4 as a dotted line, is quite similar to that found from the classical spin analysis. An important difference is that the non-collinear GGA+U calculations predict the spin-spiral state at $q_y = 0.20$ to be slightly more stable than that at $q_y = 0.95$. The spin arrangement of the spin-spiral state at $q_y = 0.20$ is illustrated in Fig. 1b and 1c. In this state of zero total spin moment, the non-collinearity of the spin arrangement occurs not only between Cu spins but also between the O and Cu spins. Our calculations show substantial moments on the O sites, as found in the previous studies.^{8,10,23} From our

calculation with $U_{eff} = 6.0$ eV, the oxygen spin moment is $0.11 \mu_B$, which agrees with the LDA+U result²⁴ and the experimental value (between 0.10 and $0.12 \mu_B$).¹⁰ Our non-collinear GGA+U electronic structure calculations with $U_{eff} > 6$ eV or with $U_{eff} < 6$ eV still show that the ground state is a spin-spiral state. Thus, with any reasonable U value, we predict a spin-spiral ground state for Li_2CuO_2 .

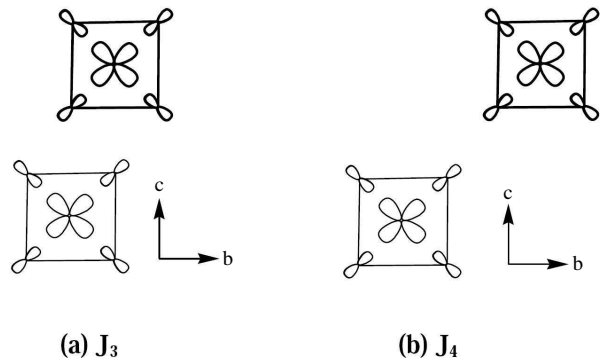


FIG. 3: Arrangements of the CuO_4 squares and their magnetic orbitals associated with (a) the NN interchain interaction J_3 and (b) the NNN interchain interaction J_4 . The two adjacent CuO_2 ribbon chains differ in their a-axis heights by $a/2$. The CuO_4 squares with different a-axis heights are indicated by thick and thin lines.

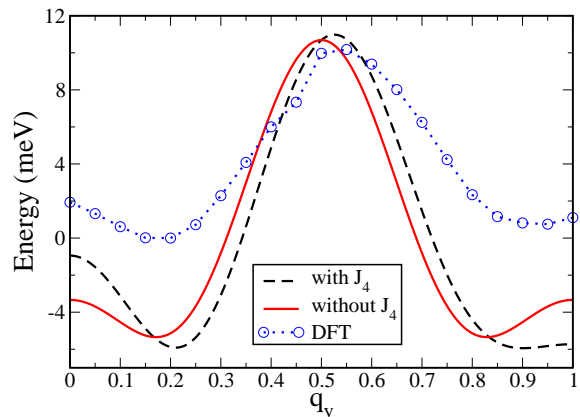


FIG. 4: (Color online) $E(0, q_y, 0)$ vs. $(0, q_y, 0)$ relations calculated for Li_2CuO_2 . The solid and dashed lines are based on the classical spin analysis (solid line: only with the intrachain interactions J_1 and J_2 , dashed line: with the intrachain interactions J_1 and J_2 as well as the interchain interaction J_4). The dotted line is based on non-collinear GGA+U calculations with $U_{eff} = 6$ eV, where the circles represent the calculated points.

From our non-collinear GGA+U calculations, the energy difference between the spin-spiral state at $\mathbf{q} = (0, 0.20, 0)$ and AFM-I state at $\mathbf{q} = (0, 1.00, 0)$ is very small (Fig. 4). In the case of $U_{eff} = 6$ eV, the difference is 1 meV/Cu and decreases with increasing U_{eff} . From the classical spin analysis shown in Fig. 4, this energy

difference is even smaller. As already pointed out, the $E(0, q_y, 0)$ vs. $(0, q_y, 0)$ curve is sharp around $q_y = 0.20$ but nearly flat around $q_y = 0.90 - 1.00$. As a consequence, the states in the region of $q_y = 0.90 - 1.00$ are nearly degenerate, and are only slightly less stable than the spin-spiral ground state at $q_y \sim 0.20$, namely, the density of states is much higher in the region of the AFM-I state than around the spin-spiral ground state. The latter provides a natural explanation for why the CuO_2 ribbon chains of Li_2CuO_2 do not exhibit a spiral-magnetic order despite that the CuO_2 chains are very similar in structure to those found in LiCu_2O_2 and LiCuVO_4 , and Li_2CuO_2 has a spin-spiral ground state. In short, the AFM-I structure ($q_y = 1.00$) is a collinear order arising

from the occupation of many nearly degenerate states around $q_y = 0.90 - 1.10$, and hence is an example of order-by-disorder.^{11,12} The phase transition below 2.4 K, believed to be a transition to a spin canted state, might arise from an increased population of the spin-spiral state at $\mathbf{q} = (0, 0.20, 0)$. What distinguishes Li_2CuO_2 from LiCu_2O_2 and LiCuVO_4 is the NNN interchain interaction J_4 , which lowers the energy of the states around the AFM-I state and makes them nearly degenerate.

Our work was supported by the Office of Basic Energy Sciences, Division of Materials Sciences, U. S. Department of Energy, under Grant No. DE-FG02-86ER45259. We thank Dr. D. Dai for useful discussions.

-
- * Corresponding author. E-mail: mike_whangbo@ncsu.edu
- ¹ S. Park, Y. J. Choi, C. L. Zhang, and S-W. Cheong, *Phys. Rev. Lett.* **98**, 057601 (2007).
 - ² Y. Naito, K. Sato, Y. Yasui, Y. Kobayashi, Y. Kobayashi, and M. Sato, *J. Phys. Soc. Jpn.* **76**, 023708 (2007).
 - ³ R. Bursill, G. A. Gehring, D. J. J. Farnell, J. B. Parkinson, T. Xiang, and C. Zeng, *J. Phys.: Condens. Matter* **7**, 8605 (1995).
 - ⁴ F. Sapiña, J. Rodríguez-Carvajal, M.J. Sanchis, R. Ibáñez, A. Beltrán, and D. Beltrán, *Solid State Commun.* **74**, 779 (1990).
 - ⁵ C. de Graaf, I. de P.R. Moreira, F. Illas, Ó. Iglesias, and A. Labarta, *Phys. Rev. B* **66**, 014448 (2002).
 - ⁶ M. Boehm, S. Coad, B. Roessli, A. Zheludev, M. Zolliker, P. Boni, D. McK. Paul, H. Eisaki, N. Motoyama, and S. Uchida, *Europhys. Lett.* **43**, 77 (1998).
 - ⁷ Y. Mizuno, T. Tohyama, and S. Maekawa, *Phys. Rev. B* **60**, 6230 (1999).
 - ⁸ U. Staub, B. Roessli, and A. Amato, *Physica B* **289-290**, 299 (2000).
 - ⁹ R. J. Ortega, P. J. Jensen, K. V. Rao, F. Sapina, D. Beltran, Z. Iqbal, J. C. Cooley, and J. L. Smith, *J. Appl. Phys.* **83**, 6542 (1998).
 - ¹⁰ E. M. L. Chung, G. J. McIntyre, D. M. Paul, G. Balakrishnan, and M. R. Lees, *Phys. Rev. B* **68**, 144410 (2003).
 - ¹¹ D. Bergman, J. Alicea, E. Gull, S. Trebst, and L. Balents, *Nat. Phys.* **3**, 487 (2007).
 - ¹² J. Villain, R. Bidaux, J. P. Carton, and R. Conte, *J. Physique* **41**, 1263 (1980).
 - ¹³ J. E. Greedan, *J. Mater. Chem.* **11**, 37 (2001).
 - ¹⁴ P. Blaha, K. Schwarz, G. Madsen, D. Kvasnicka, and J. Luitz, in *WIEN2K, An Augmented Plane Wave Plus Local Orbitals Program for Calculating Crystal Properties*, edited by K. Schwarz (Techn. Universität Wien, Austria, 2001).
 - ¹⁵ J. P. Perdew, K. Burke, and M. Ernzerhof, *Phys. Rev. Lett.* **77**, 3865 (1996).
 - ¹⁶ Our LDA calculations give qualitatively similar results.
 - ¹⁷ V. I. Anisimov, I. V. Solovyev, and M. A. Korotin, M. T. Czyżyk, and G. A. Sawatzky, *Phys. Rev. B* **48**, 16929 (1993).
 - ¹⁸ R. Laskowski, G. K. H. Madsen, P. Blaha, and K. Schwarz, *Phys. Rev. B* **69**, 140408 (2004).
 - ¹⁹ M.-H. Whangbo, H.-J. Koo and D. Dai, *J. Solid State Chem.* **176**, 417 (2003).
 - ²⁰ M. J. Freiser, *Phys. Rev.* **123**, 2003 (1961).
 - ²¹ D. Dai, H.-J. Koo, and M.-H. Whangbo, *Inorg. Chem.* **43**, 4026 (2004).
 - ²² L. M. Sandratskii, *Adv. Phys.* **47**, 91 (1998).
 - ²³ R. Weht and W. E. Pickett, *Phys. Rev. Lett.* **81**, 2502 (1998).
 - ²⁴ D. Mertz, R. Hayn, I. Opahle, and H. Rosner, *Phys. Rev. B* **72**, 085133 (2005).